ChemPubSoc Europe
DOI: 10.1002/chem.201603060
CHEMISTRY
A European Journal
Full Paper

Binuclear Complexes

Redox and Acid–Base Properties of Binuclear 4-Terphenyldithiophenolate Complexes of Nickel

Felix Koch, Andreas Berkefeld,* Hartmut Schubert, and Claudius Grauer[a]

Abstract: This work reports on the redox and acid–base properties of binuclear complexes of nickel from 1,4-terphenyldithiophenol ligands. The results provide insight into the cooperative electronic interaction between a dinickel core and its ligand. Donor/acceptor contributions flexibly adjust to stabilize different redox states at the metals, which is relevant for redox reactions like proton reduction. Proton transfer to the $[S_2Ni_2]$ core and Ni–H bond formation are kinetically favored over the thermodynamically favored yet unproductive proton transfer to ligand.

Introduction

The search for complexes of earth-abundant 3rd-row transition-metals that can mediate H–H bond formation from protons and electrons is a vibrant field of research.[1] The efficacy of sequential electron- and proton-transfer steps can be fine-tuned through ligand design. For example, it has been recognized that proximal basic substituents act as intramolecular relays for fast proton transfer to a metal or metal-H site.[2]

Thiolates are a special class of ligands in this regard. The comparatively high covalent character of metal–thiolate bonds and thiolate basicity are the elements that support intramolecular electron and proton transfer,[3] and examples have been reported for thiolate complexes of Mo,[4] Fe,[5] Ru,[6] Co,[7] Rh,[8] and Ni.[9] In fact, proton- and $(\mu\text{-S})_2$-binding by thiolate residues are among the key factors that contribute to the function of [NiFe] hydrogenase.[10] Reactivity studies of model complexes with bimetallic $(\mu\text{-S})_2Fe_2$[11] and $(\mu\text{-S})_2NiFe$[12] cores have provided detailed insight into the structure–function relationship of the active-site chemistry of this class of metalloproteins.

Among the 3d-metals, mononuclear complexes of Ni have been studied extensively for proton reduction,[13] whereas studies of homodinuclear complexes are rare.[14] Castillo reported on an *N*,*N*-bis(2-thiophenol)methylisopropylamine that binds Ni^{II} in the form of a dimeric thiolate-bridged complex. Electrochemical reduction (oxidation) of the di-Ni^{II} precursor in THF has been suggested to afford di-Ni^{I} (di-Ni^{III}) species that initiate electrocatalytic proton reduction (evolution) from HBF_4 (borohydride),[14e] as shown in Scheme 1. Although neither of the Ni species has been substantially characterized, these findings add to the general notion that low- and high-valent binuclear complexes of Ni play a role in a variety of reactions.[15]

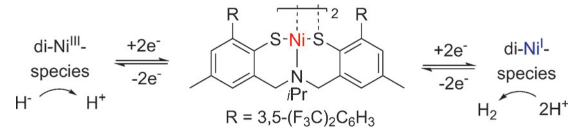

Scheme 1. Electrochemical generation of putative di-Ni^{I} or di-Ni^{III} species from a $(\mu\text{-S})_2Ni^{II}_2$ complex for electrocatalytic reduction and evolution of protons.[14e]

The structural and electronic properties of the ligands are of profound importance in this context since the metals cycle between at least two redox states during substrate turnover. A flexible adjustment of donor and acceptor contributions in metal–ligand bonding may accommodate changes of the stereoelectronic preferences of the metals[16] and provide means to manipulate their reactivity. Conjugated π-systems have been recognized to act as electronically flexible donor/acceptor ligands to single and multiple metals,[17] which includes examples of bimetallic complexes of Ni.[18] The terphenyldiphosphine ligands introduced by Agapie combine this property with strongly σ-donating phosphines. Notable examples include mono-,[19] di-,[15c] and trinuclear[20] complexes of Ni, dinuclear d^9-Pd,[20b,21] M_2-carbonyl cores of Fe, Co, and Ni,[22] and complexes of Mo in which the ligand also functions as a two-electron reservoir.[23]

We have reported on the properties of a 1,4-terphenyldithiophenol as a multidentate ligand for mono- and binuclear complexes of Ni. κ-S- and $(\mu\text{-S})_2$-coordination adjusts with σ-donor/π-acceptor bonding of the central π-system to stabilize Ni^{I} and Ni^{II} as shown in Scheme 2.[24] Although the electronic ground state structures are different, the total number of electrons is the same. Whereas complexes $\mathbf{2}_{Mes}$-L feature a $(\mu\text{-S})_2Ni^{I}_2$ core, the $(\mu\text{-}\eta^3\text{:}\eta^3\text{-}C_6H_4)Ni^{II}_2$ core in $\mathbf{1}_R$-PMe_3 results from d–π* metal-to-ligand electron transfer. Herein we report on the redox and acid–base properties of these isomeric complexes. The results

---

[a] Dipl.-Chem. F. Koch, Dr. A. Berkefeld, Dr. H. Schubert, C. Grauer
Institut für Anorganische Chemie
Eberhard Karls Universität Tübingen
Auf der Morgenstelle 18, 72076 Tübingen (Germany)
E-mail: andreas.berkefeld@anorg.uni-tuebingen.de

Supporting information for this article can be found under http://dx.doi.org/10.1002/chem.201603060.

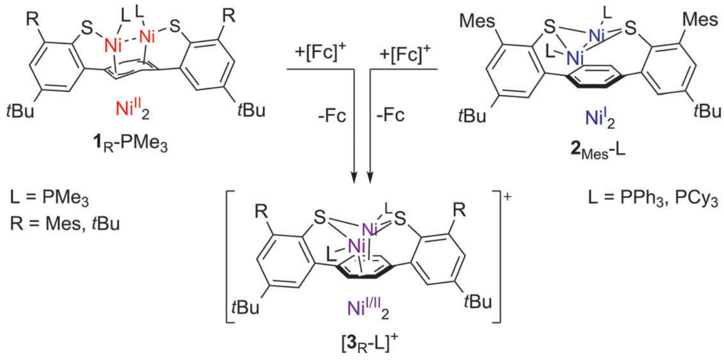

Scheme 2. Synthesis and structure of mixed-valent $Ni^{I,II}$ cations $[\mathbf{3}_R\text{-L}]^+$. Color scheme: Ni^{II} = red, $Ni^{I/II}$ = purple, Ni^I = blue; NTf$_2$-anion not shown for clarity.

show how the ligand cooperates in redox state changes and competes as a kinetically slow proton acceptor with proton reduction at the di-Ni core.

Results and Discussion

Additional insight into the variability of metal–ligand bonding has been obtained from studies of the one-electron oxidation of either type of structures shown in Scheme 2. Using the ferrocene cation, oxidation reactions are facile and cleanly produce a series of isostructural mixed-valent cations $[\mathbf{3}_R\text{-L}]^+$, which were isolated as $[N(SO_2CF_3)_2]^-$-, NTf$_2$-, salts in the form of crystalline solids. In contrast to the starting materials, compounds $\mathbf{3}_R$-L are fairly air and moisture stable, and can be manipulated in halogenated solvents other than 1,2-$C_6F_2H_4$. Characteristic electronic properties of complexes $\mathbf{3}_R$-L are collected in Table 1.

Table 1. Characteristic electronic properties of cations $[\mathbf{3}_R\text{-L}]^+$.[a]

R, L	$E_{1/2,red}/E_{1/2,ox}$[b]	λ_{max} (ε_{max})[d]	μ_{eff}[e]	$g_{iso}(g_x/\Delta g)$[f]
tBu, PMe$_3$	−980/86	738(2400)	1.8	2.109 (2.133/ 0.054)
Mes, PMe$_3$	−962/148[c]	750(1600)	2.1	2.116 (2.142/ 0.060)
Mes, PCy$_3$	−947/177	814(1600)	2.3	2.123 (2.136/ 0.047)
Mes, PPh$_3$	−760/270	836(1400)	2.0	2.109 (2.132/ 0.053)

[a] In form of NTf$_2$-salts. [b] In mV vs. Fc/[Fc]$^+$ (0.03–0.4 mм, 0.1 м nBu_4NPF_6/ 1,2-$C_6H_4F_2$, 296 K, GC disc electrode (0.039 ± 0.002 cm^2). [c] Reversible at $v > 500$ mV s^{-1}. [d] ±2 nm ($\varepsilon_{max} \pm 300$/ M^{-1} cm^{-1}), THF, 296 K. [e] C_6D_6, 278–343 K. [f] 2-Me-THF, 293 K (transition at lowest field, Δg in rhombic spectra taken at 77 K).

The molecular structure of the $[\mathbf{3}_{Mes}\text{-PMe}_3]^+$ ion is shown in Figure 1,[25] and details on isostructural cations $[\mathbf{3}_{tBu}\text{-PMe}_3]^+$ and $[\mathbf{3}_{Mes}\text{-PCy}_3]^+$ are provided in the Supporting Information, Figures S14–S15.

The $(\mu\text{-S})_2Ni_2$ core displays a local C_2v symmetry. Each Ni atom adopts a tetrahedral coordination geometry with bond distances and angles to S-, P-, and C-atoms that are equal within experimental accuracy ($3\sigma \leq 0.02$ Å). Ni-S-Ni angles of 63° and a Ni–Ni distance of 2.356 Å are slightly decreased as compared to the starting materials $\mathbf{2}_{Mes}$-L[24] (65°, 2.383 Å). A comparison of the bond lengths and angles within the central π-system to those of the flanking phenyl rings that enclose dihedral angles of ≈87° indicates μ-η^2:η^2-bonding to the Ni atoms, in agreement with Ni–C distances of 2.139 and 2.150 Å.

The electronic transition $\lambda_{max}(\varepsilon_{max}$/ M^{-1} cm^{-1}) detected for $\mathbf{3}_R$-L in THF solution most likely has a CT character but the precise nature of the chromophore is yet unknown. Notably, in the case of $\mathbf{3}_{tBu}$-PMe$_3$ λ_{max} is blueshifted by only 2 nm to 740(2700) in more-polar 1,2-$C_6F_2H_4$.

Solution magnetic moments of $[\mathbf{3}_R\text{-L}]^+$ in C_6D_6 are in the 1.8–2.3 range, slightly higher than the spin-only value of 1.73 for a $S = 1/2$ system. X-Band EPR spectra in 2-Me-THF at 293 K show isotropic signals with $g_{iso} = 2.110$–2.123 and line-widths in the 10–13 G range. Frozen solutions at 77 K display rhombic spectra with g values of the transition at lowest field in the 2.142–2.132 range and $\Delta g \leq 0.060$. Hyperfine-splitting due to coupling with the ^{31}P nuclei is not resolved in any of the spectra, which indicates a tetrahedral geometry at Ni as observed in crystalline samples.[26] While the g values support a Ni-centered electron spin, the Δg values are markedly smaller than those reported for mono- and binuclear systems with localized Ni^{II}/ Ni^I sites for which Δg is > 0.1.[18a, 27] A single example has been reported for a delocalized $d^{8.5}$-$Ni_2(\mu\text{-S})_2$ core with each Ni in a supposedly square-planar coordination site of a pyridine-2,6-dimethanethiolate, and $\Delta g = 0.14$.[28] Based on the EPR and solid-state structural data, we propose a delocalized $d^{8.5}$-Ni_2 core structure for $[\mathbf{3}_R\text{-L}]^+$ to which $(\mu\text{-S})_2$-bonding likely contributes significantly.[3] On the UV/Vis timescale, however, a localized d^9-d^8-Ni_2 core structure appears to be the appropriate description since ε_{max} is significantly smaller than expected for CT transitions within delocalized electronic structures for which ε typically is $\geq 10^4$ M^{-1}cm^{-1}.[29]

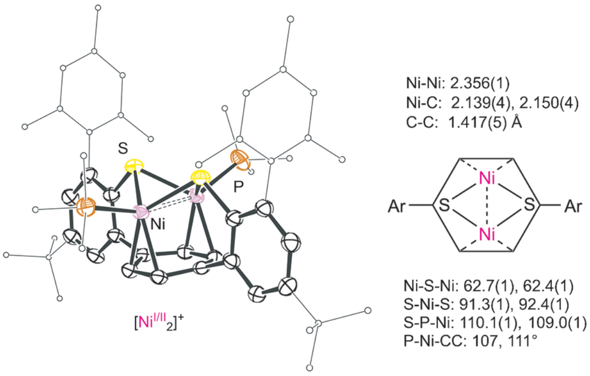

Figure 1. Molecular structure of the bimetallic cation $[\mathbf{3}_{Mes}\text{-PMe}_3]^+$: Thermal ellipsoids at 50 % probability, H-atoms and the NTf$_2$-anion are omitted for clarity.

CV analysis of $\mathbf{3}_R$-L at a glassy carbon disc electrode in 0.1 м nBu_4NPF_6/ 1,2-$C_6F_2H_4$ solution at 296 K showed that the cations are stable over a potential range of ≈1100 mV. A cathodic potential sweep vs. Fc/[Fc]$^+$ displayed electrochemically reversible reductions of cations $[\mathbf{3}_R\text{-L}]^+$ ($E_{1/2,red}$ in Table 1) to neutral complexes in all cases, with peak-potential differences of less than 70 mV and peak-current ratios i_p(red)/i_p(ox) close to unity. In addition, a second electrochemically reversible oxidation ($E_{1/2,\mathrm{ox}}$ in Table 1) to dicationic species occurs at potentials moderately positive vs. Fc/[Fc]$^+$. This second oxidation of $[\mathbf{3}_\mathrm{R}\text{-L}]^+$ presumably produces a di-Ni$^{\mathrm{II}}$ core that is stabilized through tighter μ-η^2:η^2-bonding of the ligand. In comparison to the complexes with a trialkylphosphine donor, the relative shift of half-potentials of ≈200 mV in the case of $\mathbf{3}_\mathrm{Mes}$-PPh$_3$ reflects that PPh$_3$ is a weaker σ-donor. Notably, CV data of neutral $\mathbf{1}_\mathrm{R}$-PMe$_3$ and $\mathbf{2}_\mathrm{Mes}$-L match those of $\mathbf{3}_\mathrm{R}$-L precisely, which proves the identity of the species generated in electrochemical experiments.

The fact that neutral di-Ni complexes can be oxidized twice is important with regard to their acid–base reactivity. Treatment with the cationic acid $[C_6H_5NMe_2H]^+$ in THF, with a pK_a(THF) of ≈7.39,[30] at room temperature affords the isostructural cations $[\mathbf{4}_\mathrm{R}\text{-L}]^+$ depicted in Scheme 3. The products were isolated in the form of dark red or purple, crystalline NTf$_2$-salts, with $\lambda_{\max}$ ($\varepsilon_{\max}$/M^{-1} cm^{-1}) that are 680 (3200) for $\mathbf{4}_{t\mathrm{Bu}}$-PMe$_3$, 673 (2200) for $\mathbf{4}_\mathrm{Mes}$-PMe$_3$, and 742 (2300) for $\mathbf{4}_\mathrm{Mes}$-PPh$_3$ at 296 K in THF. Compounds $\mathbf{4}_\mathrm{R}$-L are fairly stable to air and moisture and tolerate chlorinated solvents.

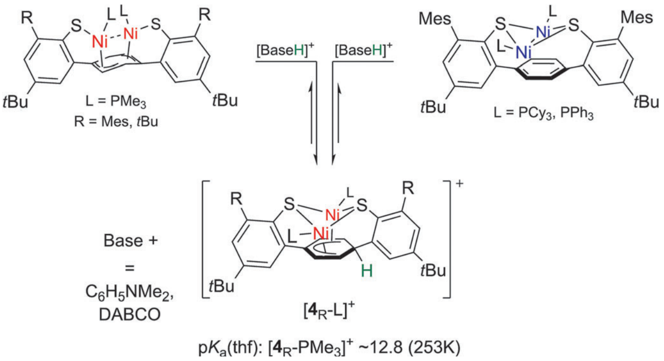

Scheme 3. Acid/base chemistry of di-Ni complexes toward cationic acids in THF; NTf$_2$-anion omitted for clarity, DABCO = 1,4-diazabicyclo[2.2.2]octane.

Formation of $[\mathbf{4}_\mathrm{R}\text{-L}]^+$ results from an intermolecular proton transfer to the C$_{\mathrm{ipso}}$-atom of the central π-system of the starting material. Indicative of a C_S-symmetric structure, ^{1}H and ^{13}C NMR spectra of, for example, $[\mathbf{4}_{t\mathrm{Bu}}\text{-PMe}_3]^+$ display resonances at 6.057/70.42 and 4.062/88.05 ppm for the μ-η^2:η^2-cyclohexadienide moiety as well as at 1.584/48.83 ppm for the *exo*-C–H bond. Characteristic sets of ^{1}H-AA′X$_9$X′$_9$ and ^{13}C{^{1}H}-ABX *N*-line patterns at 1.243/15.71 ppm imply *trans*-disposition of the PMe$_3$ ligands along the Ni–Ni vector and strong scalar P–P coupling with $J_{\mathrm{P-P}} \gg {}^{2,n}J_{\mathrm{H-P}}$ and ${}^{1,n}J_{\mathrm{C-P}}$.

The molecular structure of $[\mathbf{4}_\mathrm{Mes}\text{-PMe}_3]^+$ is shown in Figure 2 and agrees with solution structural data. Isostructural $[\mathbf{4}_\mathrm{Mes}\text{-PPh}_3]^+$ is shown in Figure S13, Supporting Information.[25]

The Ni atoms each adopt a tetrahedral coordination geometry and are chemically equivalent. The μ-η^2:η^2-cyclohexadienide moiety features a tertiary sp^3-C-atom of distorted tetrahedral geometry and bond distances of ≥1.48 Å as compared to the other four C–C bonds (≤1.43 Å) that form a delocalized π-system. The structural parameters of the cyclohexadienide fragment are similar to those found in a mononuclear complex of Ni$^{\mathrm{II}}$ reported by Agapie.[19] The local structure at the Ni atoms is similar to that in $[\mathbf{3}_\mathrm{R}\text{-L}]^+$, although shorter Ni–C distances of 2.045(3) and 2.052(3) Å are indicative of the higher oxidation state of +2 in $[\mathbf{4}_\mathrm{R}\text{-L}]^+$.[18b,24] The diamagnetism of $[\mathbf{4}_\mathrm{R}\text{-L}]^+$ must result from antiferromagnetic coupling of the $S = 1$ Ni$^{\mathrm{II}}$ sites, and is probably mediated through (μ-S)$_2$- and μ-η^2:η^2-bonding to the ligand.

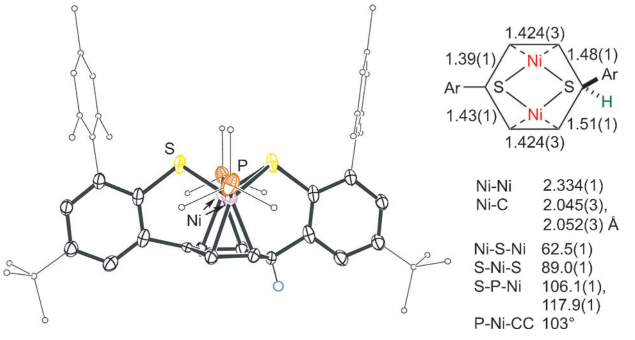

Figure 2. Molecular structure of $[\mathbf{4}_\mathrm{Mes}\text{-PMe}_3]^+$: Thermal ellipsoids at 50% probability, H-atoms, lattice-solvent, and the NTf$_2$-anion are omitted for clarity.

Quantitative ^{2}H NMR spectroscopic monitoring of the reaction of $\mathbf{1}_\mathrm{Mes}$-PMe$_3$ and >90 D-% $[C_6H_5NMe_2D]^+$ to [D$_1$]-$[\mathbf{4}_\mathrm{Mes}\text{-PMe}_3]^+$ in THF verified the regioselectivity of the H$^+$-transfer to the ligand. No introduction of the D-label into any of the olefinic positions was observed. Alternative formation of a putative [Ni$_2$D]$^+$-species that undergoes intramolecular D-migration to the proximal π-system of the ligand either is not favorable or reversible. Addition of one equivalent of 1,4-diazabicyclo[2.2.2]octane (DABCO) produces an equilibrium mixture of $\mathbf{1}_\mathrm{Mes}$-PMe$_3$ (85%), $[\mathbf{4}_\mathrm{Mes}\text{-PMe}_3]^+$ (15%), and rapidly exchanging free and protonated base. The reverse reaction yields a mixture of equal composition. Equilibrium concentrations of $\mathbf{1}_\mathrm{Mes}$-PMe$_3$ and $[\mathbf{4}_\mathrm{Mes}\text{-PMe}_3]^+$ were estimated at 253 K as a function of added [DABCOH]$^+$, which provided a pK_a(THF) of ≈12.8 for cations $[\mathbf{4}_\mathrm{R}\text{-PMe}_3]^+$.

Interestingly, solution X-band EPR spectra of crude $\mathbf{4}_\mathrm{R}$-L verified co-formation of $\mathbf{3}_\mathrm{R}$-L, albeit at low quantities of <5% as judged from ^{1}H NMR spectra. Substitution of the 4-position in $[C_6H_5NMe_2H]^+$ for acetyl or NO$_2$ increases pK_a(THF) values of the cationic acid by about three orders of magnitude.[30] As the result, the molar fraction of $[\mathbf{4}_\mathrm{Mes}\text{-PMe}_3]^+$ decreases in favor of $[\mathbf{3}_\mathrm{Mes}\text{-PMe}_3]^+$ as the ultimate product as shown in Table 2. The formation of H$_2$ as a byproduct was verified by monitoring the reaction by ^{1}H NMR spectroscopy. Ultrasound treatment and readdition of H$_2$ to NMR tubes by syringe verified its identity, while use of a 1:2 mixture of HNTf$_2$/DNTf$_2$ resulted in H–D formation. In other words, acids react as one-electron oxidants with neutral $\mathbf{1}_\mathrm{R}$-PMe$_3$, depending on their pK_a. In fact, substitution of [Fc]NTf$_2$ for HNTf$_2$ in the bulk reaction of Scheme 2 provides salts $\mathbf{3}_\mathrm{R}$-PMe$_3$ in identical isolated yields and purity.

To explain the dependence of chemoselectivity on acid strength in mechanistic terms requires knowledge as to wheth-

Table 2. Chemoselectivity of the reaction of $\mathbf{1}_{Mes}$-PMe$_3$ with cationic acids[a].

Acid (pK_a(THF))[b]	n($\mathbf{4}_{Mes}$-PMe$_3$)[e]	1,5-COD %-isomerization[f]
[DABCOH]$^+$ ($\approx$13.7)[30]	0.15	2 (1 h), 50 (44 h), 65 (74 h)
[$C_6H_5NMe_2H$]$^+$ (7.39)[30]	$>$0.95	6
[4-Acetyl-$C_6H_5NMe_2H$]$^+$[c]	0.43	not tested
[4-NO_2-$C_6H_5NMe_2H$]$^+$ ($\approx$5)[d]	$<$0.05	not tested
$HN(SO_2CF_3)_2$ ($<$5)[c]	$<$0.05	$>$98

[a] [D8]THF, 10 equiv 1,5-COD, 1.3 equivalents of acid added at 193 K, slow warming to room temperature within 2 h. [b] NTf_2-salts. [c] No pK_a(THF) values available. [d] Estimated from pK_a(THF) of anilinium acids.[30] [e] Reactions in the absence of 1,5-COD, values calculated from ^{1}H NMR spectra. [f] Molar fraction of 1,4-/ 1,3- vs. 1,5-COD derived from ^{1}H NMR and GCMS data.

er [Ni$_2$H]-species are accessible under the reaction conditions. As an internal chemical probe for Ni–H bond formation, the isomerization of additionally added 1,5-COD (1,5-COD = 1,5-cyclooctadiene) to the thermodynamically more stable 1,4- and 1,3-isomers was studied. Reactions were run in the presence of 10 equivalents of 1,5-COD under otherwise identical conditions, and the reaction mixtures subject to mass spectrometric (GCMS) analysis. As described in Table 2, the reaction of $\mathbf{1}_{Mes}$-PMe$_3$ with HNTf$_2$ produced an 1:12:87 mixture of 1,5-, 1,4-, and 1,3-COD, [$\mathbf{4}_{Mes}$-PMe$_3$]$^+$ now being the major product ($\approx$90%) along with some [$\mathbf{3}_{Mes}$-PMe$_3$]$^+$ ($<$10%). Most intriguingly, a small but significant quantity of 6% of 1,4-COD was generated in the reaction with [$C_6H_5NMe_2H$]$^+$. An even continuous isomerization was observed for [DABCOH]$^+$, reaching 65% of 1,4- and 1,3-COD in a 4:1 ratio after 74 h at room temperature. Control experiments verified that the isomerization of 1,5-COD requires both $\mathbf{1}_{Mes}$-PMe$_3$ and acid. [Ni(cod)$_2$] as a substitute for $\mathbf{1}_{Mes}$-PMe$_3$ rapidly produced Ni-black and a sub-stoichiometric quantity of 1,n-COD (n = 3, 4). Formation of Ni-black is not significant in reactions of $\mathbf{1}_{Mes}$-PMe$_3$.

The isomerization of 1,5-COD indicates that [Ni$_2$H]-species are present in mixtures of $\mathbf{1}_R$-PMe$_3$ and any of the cationic acids, and likely form reversibly since COD-isomerization ceases once the formation of [$\mathbf{4}_{Mes}$-PMe$_3$]$^+$ is complete. The dependence of both the chemoselectivity of the oxidation of $\mathbf{1}_{Mes}$-PMe$_3$ to $\mathbf{3}_{Mes}$-PMe$_3$ and the extent of COD-isomerization on acid pK_a requires that the formation of putative [Ni$_2$H]$^+$-species is kinetically favored over that of ligand protonated $\mathbf{4}_{Mes}$-PMe$_3$ which is the thermodynamic product. To verify whether H$_2$ formation requires the intermediate formation of $\mathbf{4}_R$-L, $>$90 D-% selectively labelled [D$_1$]-[$\mathbf{4}_{tBu}$-PMe$_3$]$^+$ was treated with the strong cationic acid [4-NO_2-$C_6H_4NMe_2H$]$^+$ as well as with an 1:1 mixture of the acid and its conjugate base at room temperature as shown in Scheme 4, I. EPR and ^{1}H NMR spectroscopic monitoring showed no significant conversion into either [$\mathbf{3}_{tBu}$-PMe$_3$]$^+$, which is the ultimate product from H$_2$ formation or [$\mathbf{4}_{tBu}$-PMe$_3$]$^+$ from a net D–H exchange. As summarized in Scheme 4, II these results provide a strong indication that H$_2$ formation involves acid-generated [Ni$_2$H]$^+$-species and that reversible proton transfer to the ligand is a competitive yet slow side reaction.

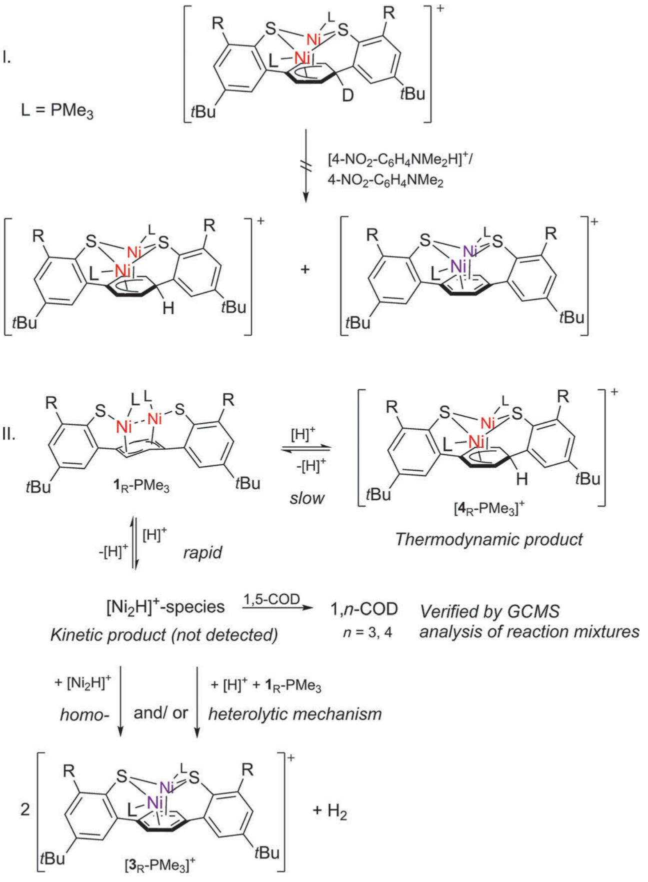

Scheme 4. I: Reaction of cationic acids with selectively deuterated [D$_1$]-[$\mathbf{4}_{tBu}$-PMe$_3$]NTf$_2$. II: Overview on the acid/base chemistry of $\mathbf{1}_R$-PMe$_3$.

Conclusions

Comparison of the electronic structures of isomeric compounds $\mathbf{1}_R$-PMe$_3$ and $\mathbf{2}_{Mes}$-L illustrates how a flexible adjustment of donor/acceptor components allows for manipulating the redox state of nickel. In the cations [$\mathbf{3}_R$-L]$^+$ the μ-η^2:η^2-coordination of the π-system compensates for the lack of electron density at Ni. In contrast to compounds $\mathbf{2}_{Mes}$-L that already possess a rhombic (μ-S)$_2$Ni$_2$ core structure, oxidation of di-Ni^{II} complexes $\mathbf{1}_R$-PMe$_3$ involves a rearrangement of the ligand field from square-planar to tetrahedral. However, the half-potentials for the first oxidation of neutral $\mathbf{1}_{Mes}$-PMe$_3$ and $\mathbf{2}_{Mes}$-PCy$_3$ differ by only 15 mV (see $E_{1/2,red}$ in Table 1), and in both cases the reactions are diffusion controlled for scan rates $\leq$5000 mV s^{-1}. So despite being substantial, the reorganization of the ligand field appears to impose only a small kinetic barrier to oxidation. The electrochemically reversible second oxidation to dicationic species is assumed to further strengthen the μ-η^2:η^2-coordination of the π-system with Ni-arene bond metrics that presumably are similar to those determined in [$\mathbf{4}_R$-L]$^+$.

The formation of ligand protonated [$\mathbf{4}_R$-L]$^+$ results in a significant change of the structural and electronic properties of the central π-system, and restoration of aromaticity likely provides a driving force for the reversibility of this reaction. On the other hand, the rate of proton transfer to the π-system is lower than that of the formation of putative [Ni$_2$H]$^+$-species.

Since direct proton transfer to a low valent metal is expected to be kinetically slow,[11b,31] we propose a rapid pre-equilibrium proton transfer to thiolate prior to Ni–H bond formation, in an analogous fashion to what has been described for mono- and binuclear complexes of Ni and Fe with a pendant amine group in close proximity to the metal site(s).[1c,11c]

Regarding the mechanism of H_2-formation from $[Ni_2H]^+$-species, homo- and heterolytic pathways have to be taken into account as summarized in Scheme 4, II. These mechanisms are well established for Co–H fragments such as $[Co^{III}H]^+$ and neutral $[Co^{II}H]$,[32] and have also been evoked for Ni–H species,[13b] but additional insight into the formation and properties of acid-generated $[Ni_2H]^+$-species is required.

In summary, the redox and acid–base properties of binuclear complexes of Ni of 1,4-terphenyldithiophenol ligands have been studied. The results reported herein demonstrate that a fine balance of donor/ acceptor contributions in ligand-to-metal bonding allows for stabilizing different redox states in the context of chemical processes such as proton reduction, as well as controlling the overall rates of competing reaction pathways.

Experimental Section

General

All manipulations of air- and moisture-sensitive compounds were carried out under an atmosphere of dry argon using standard Schlenk or glove-box techniques. Starting materials $\mathbf{1}_{Mes}$-PMe_3 and $\mathbf{2}_{Mes}$-L,[24] $(Me_3P)_2NiCl_2$,[33] and $[Ni(cod)_2]$[34] were prepared by following literature procedures. Protocols for the preparation of *t*Bu-substituted 1,4-terphenyldithiophenol, $\mathbf{1}_{tBu}$-PMe_3, and all cationic acids are provided in the Supporting Information. *N*,*N*-Dimethylthiocarbamoyl chloride (Acros Organics) was used as received and stored in a desiccator over P_2O_5. Bis(trifluoromethanesulfonyl)amine ($HNTf_2$, 99%, Acros Organics) was sublimed once before use. $AgClO_4$ and high-purity ferrocene (Fc) were obtained from Alfa Aesar, and Fc was sublimed once prior to use. D_2SO_4 (>98% in 99.9+ % D_2O) was obtained from ABCR. Benzoquinone was recrystallized three times from ethanol, sublimed twice (room temperature, 10^{-3} mbar, static vacuum), and stored under argon. Solvents were purified and dried prior to use. Dichloromethane and hexane were dried using an MBraun solvent purification system (SPS). Benzene, diethyl ether, pentane, THF, and toluene were predried over activated 3 Å molecular sieves and distilled from sodium benzophenone ketyl or potassium metal under argon. 2-Methyl-tetrahydrofuran (2-Me-THF, >99%, inhibitor free, Sigma Aldrich) was dried over and distilled from NaK alloy and stored in the glove box. Methanol, *N*,*N*-dimethylformamide, *N*-methyl-2-pyrrolidone, and 1,2-difluorobenzene (1,2-DFB) were dried and purified by percolation through a column of activated neutral alumina, and 1,2-DFB was distilled onto fresh alumina prior to use in electrochemical experiments. Acetonitrile (MeCN) for use in electrochemical experiments was sequentially dried over and distilled from CaH_2 and P_2O_5, and finally percolated through activated neutral alumina. C_6D_6 and [D8]THF were dried over and distilled from NaK alloy. Hexamethyldisiloxane (HMDS), $CDCl_3$, and CD_2Cl_2 were dried over and vacuum transferred from 3 Å molecular sieves. All solvents were stored over 3 Å molecular sieves or activated neutral alumina (MeCN, 1,2-DFB) under argon. Molecular sieves and neutral alumina were activated by heating under dynamic vacuum (10^{-3} mbar) at 250 °C for 24–48 hours. NMR data were recorded on Bruker Avance II 400 and DRX 250 instruments. VT NMR spectra were collected on a Bruker AVII+500 spectrometer. δ values are given in ppm, *J* values in Hz. ^1H and $^{13}C\{^1H\}$ NMR chemical shifts are referenced to the residual ^1H and naturally abundance ^{13}C resonances of the solvents: $\delta = 7.16/\ 128.06$ (C_6D_6), 1.72/ 67.21 ([D8]THF), 5.32/ 53.84 (CD_2Cl_2), and 7.26/ 77.16 ppm ($CDCl_3$). ^{31}P NMR chemical shifts are referenced to an external standard sample of 85% H_3PO_4 set to $\delta = 0$ ppm. EPR spectra were collected using 4 mm O.D. Wilmad quartz (CFQ) EPR tubes on a continuous wave X-band Bruker ESP 300E spectrometer, and are referenced to the Bruker Strong Pitch standard $g_{iso} = 2.0028$. Whenever applicable, reactions were monitored by GCMS analysis on a HP 6890 instrument equipped with a DB-5MS capillary column (JW, 30 m × 250 μm × 0.25 μm) and a MSD 5973 mass detector. Samples were filtered through activated alumina prior to GCMS analysis. Evan's method[35] was employed to determine μ_{eff} in solution using a coaxial insert for 5 mm NMR sample tubes, $\chi_M^{dia} = -0.5 \times M$, M = unitless molecular weight of the sample,[36] and $\chi_M^{dia}(\text{benzene}) = -5.47 \times 10^{-5}\ cm^3\,mol^{-1}$[37] were used to correct for diamagnetic susceptibilities of sample and solvent.

X-ray data were collected on a Bruker Smart APEXII diffractometer with graphite-monochromated $Mo_{K\alpha}$ radiation. The programs used were Bruker's APEX2 v2011.8-0, including SADABS for absorption correction and SAINT for structure solution, the WinGX suite of programs version 2013.3,[38] SHELXS and SHELXL for structure solution and refinement,[39] PLATON,[40] and Ortep.[41] Crystals were, unless otherwise noted, coated in a perfluorinated polyether oil and mounted on a 100 μm MiTeGen MicroMounts™ loop that was placed on the goniometer head under a stream of dry nitrogen at 100 K.

CV measurements were performed at room temperature (296 K) under an argon atmosphere with an ECi 200 potentiostat (Nordic Electrochemistry) in a gas-tight, full-glass, three-electrode cell setup. nBu_4NPF_6 was used as electrolyte (Alfa Aesar), was recrystallized 3 times from acetone/water and employed as a 0.1 M solution in 1,2-DFB and MeCN. The potentiostat was controlled using the EC4™ DAQ (version 4.1.90.1, Nordic Electrochemistry) software, and data were treated with EC4™ VIEW (version 1.2.36.1, Nordic Electrochemistry). A GC disc electrode (Metrohm, electro-active area = $0.039 \pm 0.002\ cm^2$) and a 1 mm coiled Pt-wire were employed as working and counter electrodes. The Ag/Ag$^+$ redox couple, in the form of a 0.5 mm Ag wire in a 0.01 M $AgClO_4$/ 0.1 M nBu_4NPF_6 MeCN solution, served as a reference electrode. Voltammograms were corrected for capacitive currents of electrolyte solutions and overall cell resistance, and potentials are reported relative to Fc/[Fc]$^+$ in 1,2-DFB, with $E_{1/2}$(Fc/[Fc]$^+$/0.1 M nBu_4NPF_6/ 1,2-DFB, 296 K) = 0.222 ± 0.003 mV. The electroactive area of the GC disc electrode was calculated from Fc/[Fc]$^+$ measurements in 0.1 M nBu_4NPF_6 solution in MeCN at various concentrations and potential sweep rates, using D(Fc/MeCN, 293 K) = $2.40 \times 10^{-5}\ cm^2\,s^{-1}$. The working electrode was rinsed with acetone, polished very gently with a paste of 0.3 μm alumina (Metrohm) in deionized water, rinsed thoroughly with plenty of deionized water, and finally acetone after each use and stored in a desiccator over P_2O_5. Periodic Fc/[Fc]$^+$ reference measurements verified the electroactive surface area of the GC electrode, and the stability of the potential of the Ag/Ag$^+$ reference electrode.

Numeration scheme used for ligands $[Mes_2tBu_2S_2]^{2-}$ and $[tBu_4S_2]^{2-}$ in coordination compounds:

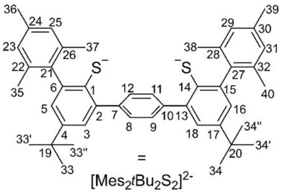

= $[Mes_2tBu_2S_2]^{2-}$

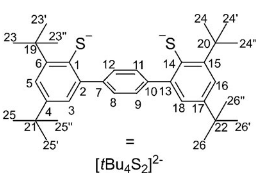

= $[tBu_4S_2]^{2-}$

Synthesis and characterization

Preparation of ferrocenium bis(trifluoromethanesulfonyl)imide [Fc]NTf$_2$: To a solution of 4-benzoquinone (87 mg, 0.81 mmol) in diethyl ether was first added dropwise a solution of HNTf$_2$ (476 mg, 1.693 mmol) in diethyl ether at room temperature, followed by a diethyl ether solution of ferrocene (250 mg, 1.344 mmol); the total volume was 25 mL. A green microcrystalline solid separated immediately after complete addition of ferrocene, and the supernatant solution was removed by cannula. The resulting green solid was washed with diethyl ether and dried under dynamic vacuum to afford 574 mg (1.23 mmol, 92 %) of blue/green microcrystals. UV/Vis (THF): λ_{max} (ε_{max}) = 622 nm (530 mol−1dm3 cm−1); ESI MS: *m/z*: 185.9 [M^+], 279.7 [M^-]; elemental analysis calcd (%) for $C_{12}H_{10}F_6FeNO_4S_2$: C 30.92, H 2.16, N 3.00, S 13.75; found: C 31.00, H 2.14, N 3.10, S 13.78.

Preparation of [3$_{tBu}$-PMe$_3$]NTf$_2$

Procedure A: A solution of **1**$_{tBu}$-PMe$_3$ (100 mg, 0.127 mmol) in 6 g of THF at −40 °C was cannula transferred onto solid [Fc]NTf$_2$ (59 mg, 0.127 mmol) precooled at −40 °C. The reaction mixture turned dark red immediately and was slowly warmed to room temperature. After the solvent had been removed under dynamic vacuum, the red solid residue was dissolved in 15 mL of toluene, and the resulting dark red solution filtered and concentrated to 5 mL, which deposited dark red needles. The mixture was kept at −35 °C for 3 h, and the orange supernatant was separated from the product by cannula. Drying under dynamic vacuum produces [**3**$_{tBu}$-PMe$_3$]NTf$_2$ × 0.25C$_7$H$_8$ (109 mg, 0.100 mmol, 78 %).

Procedure B: To a solution of **1**$_{tBu}$-PMe$_3$ (50 mg, 0.064 mmol) in 10 mL of diethyl ether was added 10 mL of a diethyl ether solution of HNTf$_2$ (18 mg, 0.064 mmol) at room temperature. The color changed immediately from red to dark red/purple and the mixture was filtered after 30 min. The resulting filtrate was concentrated until [**3**$_{tBu}$-PMe$_3$]NTf$_2$ separated in the form of dark-red needles. After 3 h at −35 °C, a pale-red supernatant solution was removed by cannula, and the product dried under dynamic vacuum. Yield: 47 mg (0.044 mmol, 69 %) of dark red/purple needles.

CW X-Band EPR (2-Me-THF, 293 K): Microwave frequency 9.7580 GHz, power 5.03 mW, modulation amplitude 0.951 G, modulation frequency 100 kHz, center field 3279 G, sweep width 700 G, resolution 1024 points: g_{iso} = 2.11; 77 K, microwave frequency 9.5022 GHz: g_x = 2.133, g_y = 2.118, g_z = 2.079; UV/Vis (THF): λ (ε) = 284 (18 000), 303 (sh), 335 (sh), 387 (11 000), 470 (4700), 562 (4300), 738 nm (2400 mol^{-1} dm^3 cm^{-1}); elemental analysis calcd (%) for $C_{42}H_{62}F_6Ni_2NO_4P_2S_4 \times 0.25C_7H_8$: C 48.23, H 5.92, N 1.29, S 11.77; found: C 48.46, H 5.85, N 1.61, S 11.61; μ_{eff} = 1.8 (288–343 K, C$_6$D$_6$/HMDS).

Preparation of [4$_{tBu}$-PMe$_3$]NTf$_2$: A solution of [C$_6$H$_5$NMe$_2$H]NTf$_2$ (51 mg, 0.127 mmol) in 10 mL THF was cooled to −40 °C and cannula transferred to a solution of **1**$_{tBu}$-PMe$_3$ (100 mg, 0.127 mmol) in 10 mL THF precooled to −40 °C. After 5 min at −40 °C, warming to room temperature afforded a red/purple solution. The solvent was removed under dynamic vacuum, and the dark red residue washed with 10 mL portions of hexane two times and dried. The product was extracted into diethyl ether and the dark red solution was filtered, concentrated until crystallization started, and kept at −35 °C for 5 h. A pale red supernatant was removed by cannula, and the dark red needles dried under vacuum. Yield: 113 mg (0.106 mmol, 81 %). ^{1}H NMR (500 MHz, [D8]THF, 299 K): δ = 7.69 (d, ^4J(HH) = 2.1 Hz, 1 H, H-3), 7.52 (d, ^4J(HH) = 2.1 Hz, 1 H, H-16), 7.47 (d, ^4J(HH) = 2.3 Hz, 1 H, H-5), 7.29 (d, ^4J(HH) = 2.3 Hz, 1 H, H-18), 6.06 (m, 2 H, H-8,-12), 4.06 (m, 2 H, H-9,-11), 2.01 (s, 9 H, H-24), 1.67 (s, 9 H, H-23), 1.59 (br m, 1 H, H-10), 1.41 (s, 9 H, H-25), 1.34 (s, 9 H, H-26), 1.24 ppm (AA′X$_9$X$_9$′, J(PP) ≫ J(HP), $\Delta\nu$ (N-lines) = 9.5 Hz, 18 H, P(CH_3)$_3$); ^{13}C{^{1}H} NMR (126 MHz, CDCl$_3$, 298 K): δ = 152.74 (C-1), 151.72 (C-13), 150.44 (C-15), 150.16 (C-6), 149,47 (C-4), 148.06 (C17), 147.11 (br m, C-7), 142.94 (C-2), 127.87 (C-14), 126.53 (C18), 124.08 (C-16), 123.67 (C-5), 120.28 (quartet, ^1J(CF) = 322 Hz, NTf$_2$-anion), 118.09 (C-3), 88.05 (C-8,-12), 70.42 (C-9,-11), 48.83 (C(sp^3)-10), 37.71 (C-20), 36.8 (C-19), 34.77 (C-21), 34.46 (C-22), 30.89 (C-24), 30.62 (C-25), 30.56 (C-26), 30.1 (C-23), 15.71 ppm (ABX, J(PP) ≫ J(CP), $\Delta\nu$ (N-lines) = 28.4 Hz, P(CH$_3$)$_3$); ^{19}F NMR (376 MHz, [D8]THF, 299 K): δ−81.6 ppm (s, NTf$_2$-anion); ^{31}P{^{1}H} NMR (202 MHz, [D8]THF, 299 K): δ = −20.53 ppm; UV/Vis (THF): λ_{max} (ε): 240 (27 700), 264 (24 200), 316 (16 000), 367 (11 300), 494 (10 000), 680 nm (3200 mol^{-1} dm^3 cm^{-1}); elemental analysis calcd (%) for $C_{42}H_{63}NF_6Ni_2O_4P_2S_2$: C 47.25, H 5.95, N 1.31, S 12.01; found: C 47.12, H 5.88, N 1.38, S 11.85.

Complex [D$_1$]-[**4**$_{tBu}$-PMe$_3$]NTf$_2$ was prepared from **1**$_{tBu}$-PMe$_3$ and [C$_6$H$_5$NMe$_2$D]NTf$_2$ (> 95 D-%) following the same protocol. Yield: 110 mg (0.103 mmol, 79 %), > 95 % D-% as judged from ^{1}H NMR spectra by relative integration.

Preparation of [3$_{Mes}$-PMe$_3$]NTf$_2$: A solution of **1**$_{Mes}$-PMe$_3$ (145 mg, 0.148 mmol) in diethyl ether (40 mL) was cooled in a dry ice/acetone bath to −78 °C. A solution of HNTf$_2$ (55 mg, 0.195 mmol) in diethyl ether (10 mL) was added. The resulting mixture was allowed to gradually warm to r.t. in the cooling bath over a period of 3 h. After this time, the color of the reaction mixture changed from dark red to red brown. Crystallization was initiated by reducing the solvent by half under reduced pressure. After 12 h at 6 °C, the crystals were separated and the product recrystallized by slow diffusion of hexane vapor into a concentrated solution of [**3**$_{Mes}$-PMe$_3$]$^+$ in THF (98 mg, 55 %). The same procedure was used to obtain single crystals suitable for XRD analysis. UV/Vis (THF): λ (ε): 280 (sh), 322 (sh), 386 (7500), 475 (sh), 566 (2900), 750 nm (1590 mol^{-1} dm^3 cm^{-1}); μ_{eff} = 2.1 (Evans method, 278–318 K, C$_6$D$_6$ containing HMDS); elemental analysis calcd (%) for $C_{52}H_{67}Ni_2P_2S_4N F_6O_4$: C 52.46, H 5.59, S 10.77, N 1.18; found: C 52.14, H 5.64, S 12.18, N 1.19.

Preparation of [4$_{Mes}$-PMe$_3$]NTf$_2$: **1**$_{Mes}$-PMe$_3$ (150 mg, 0.164 mmol) and [C$_6$H$_5$NMe$_2$H]NTf$_2$ (66 mg, 0.164 mmol) were combined in a Schlenk flask and cooled in a dry ice/acetone bath to −78 °C. Diethyl ether was added slowly and the resulting reaction mixture was warmed up to room temperature over a period of 2.5 h in the cooling bath. Over this time, the color of the solution changed from dark red to red brown. The solvent was removed under vacuum and the reddish brown solid was recrystallized by slow diffusion of hexane vapor into a concentrated solution of [**4**$_{Mes}$-PMe$_3$]$^+$ in THF (60 mg, 30 %). The same procedure was used to obtain single crystals suitable for XRD analysis. ^{1}H NMR (500 MHz, [D8]THF, 299 K): δ = 7.77 (d, ^4J(H,H) = 2.16 Hz, 1 H, H-18), 7.38 (d, ^4J(H,H) = 2.26 Hz, 1 H, 3-H), 7.14 (d, ^4J(H,H) = 2.15 Hz, 1 H, H-16), 7.11

(d, ^4J(H,H) = 2.26 Hz, 1 H, H-5), 6.96 (s, 2 H, H-23,-25), 6.86 (s, 2 H, H-29,-31), 6.15 (m, 2 H, H-9,-11), 4.09 (m, 2 H, 8-, H-12), 2.29 (s, 3 H, H-36), 2.23 (s, 3 H, H-39), 2.06 (s, 6 H, H-35,-37), 1.94, (s, 6 H, H-38,-40), 1.40 (s, 1 H, H-7), 1.37 (s, 9 H, H-33), 1.30 (s, 9 H, H-34) 1.13 ppm ($AA'X_9X_9'$, $J(PP) \gg J(HP)$, $\Delta\nu$ (N-lines) = 9.5 Hz, 18 H, $P(CH_3)_3$); $^{13}C\{^1H\}$ NMR (126 MHz, [D8]THF, 299 K): $\delta = 154.0$ (C-14), 150.1 (C-17), 149.7, 148.9 (C-4), 148.4 (t, ^2J(C,P) = 2.00 Hz, C-10), 142.6, 142.5, 141.5, 139.7 (C-21), 136.6, 136.3, 135.6, 135.5, 135.4 (C-27), 129.3 (C-1), 127.7 (C-23,-25,-29,-31), 127.6 (C-16), 127.0 (C-5), 126.5 (C-3), 118.5 (C-18), 89.2 (C-9,-11), 70.0 (C-8,-12), 48.3 (C-7), 34.7 (C-19), 34.4 (C-20), 30.6 (C-33), 30.5 (C-34), 22.2 (C-36), 20.5 (C-35,-37), 20.4 (C-38,-40), 20.1 (C-39), 15.9 ppm (ABX, $J(PP) \gg J(CP)$, $\Delta\nu$ (N-lines) = 28.3 Hz, $P(CH_3)_3$); $^{31}P\{^1H\}$ NMR (202 MHz, [D8]THF, 299 K): $\delta = -19.41$ ppm; ^{19}F NMR (376 MHz, $CDCl_3$, 298 K): $\delta = -77.59$ ppm (s, NTf_2-anion); UV/Vis (THF): λ (ε): 312 (sh), 375 (7700), 497 (6100), 673 nm (2200 $mol^{-1} dm^3 cm^{-1}$); elemental analysis calcd (%) for $C_{52}H_{67}Ni_2P_2S_4NF_6O_4$: C 52.41, H 5.67, S 10.76, N 1.18; found: C 51.46, H 5.71, S 10.77, N 1.24.

Preparation of $[\mathbf{3_{Mes}}$-$\mathbf{PPh_3}]\mathbf{NTf_2}$: A solution of $\mathbf{2}_{Mes}$-PPh_3 (50 mg, 0.039 mmol) in thf (8 mL) was cooled down to $-15\,^\circ C$ in an ice/NaCl bath and an ice-cooled solution of $FcNTf_2$ (18 mg, 0.039 mmol) in THF (8 mL) was added by cannula-transfer. Instantaneously, the color of the solution turns yellow brown and the reaction mixture was stirred for 30 min in the cooling bath and for an additional 30 min. at room temperature. The solvent was removed under vacuum and the product was recrystallized from a concentrated solution in toluene at $-35\,^\circ C$. Yield 25 mg (0.016 mmol, 41 %) yellow brown crystals. UV/Vis(THF): λ (ε): 265 (sh), 315 (sh), 428 (12 200), 505 (sh), 585 (sh), 836 nm (1300 $mol^{-1} dm^3 cm^{-1}$); $\mu_{eff} = 2.0$ (Evans method, 278–318 K, C_6D_6 containing HMDS); elemental analysis calcd (%) for $C_{82}H_{78}Ni_2P_2S_4NF_6O_4$: C 63.01, H 5.03, S 8.20, N 0.90; found C 62.17, H 4.96, S 7.84, N 0.96.

Preparation of $[\mathbf{4_{Mes}}$-$\mathbf{PPh_3}]\mathbf{NTf_2}$: A solution of $\mathbf{2}_{Mes}$-PPh_3 (50 mg, 0.039 mmol) in diethyl ether (20 mL) was cooled in a dry ice/acetone bath to $-78\,^\circ C$ and a solution of $HNTf_2$ (14 mg, 0.051 mmol) in diethyl ether (10 mL) was added. The resulting mixture was allowed to gradually warm to room temperature in the cooling bath over a period of 2.5 h. After this time, the color of the reaction mixture changed from green to brown and the solvent was removed under vacuum. Bulk crystallization by slow diffusion of hexane vapor into a concentrated solution of $[\mathbf{4}_{Mes}$-$PPh_3]NTf_2$ in THF produced dark red crystals (47 mg, 77 %). The same procedure was used to obtain single crystals suitable for XRD analysis. ^1H NMR (500 MHz, [D8]THF, 299 K): $\delta = 7.92$ (d, ^4J(H,H) = 2.14 Hz, 1 H, 18-H), 7.60 (d, ^4J(H,H) = 2.07 Hz, 1 H, H-3), 7.41 (m, 6 H, H-PPh_3), 7.18 (2 H, 5-H, 16-H,)[a]), 7.17 (m, 12 H, H-PPh_3), 6.96 (m, 12 H, H-PPh_3), 6.70 (s, 2 H, H-23,-25), 6.58 (s, 2 H, H-29,-31), 6.30 (m, 2 H, H-9,-11) 4.35 (m, 2 H, H-8,-12), 2.36 (s, 3 H, H-36), 2.24 (s, 3 H, H-39), 1.67 (s, 1 H, H-7), 1.51 (s, 9 H, H-33), 1.44 (s, 9 H, H-34), 1.35 ppm (s, 6 H, H-35,-37), 1.25 (s, 6 H, H-38,-40); $^{13}C\{^1H\}$ NMR(126 MHz, [D8]THF, 299 K): $\delta =$ 153.94 (C-14), 150.98 (C-17), 149.66 (C-4), 149.37, 149.19, 144.49, 143.87, 140.98, 138.91 (C-21), 136.26, 135.94, 135.88, 135.80, 134.79 (C-27), 133.18 (C-PPh_3), 130.77 (C-PPh_3), 130.51 (C-5), 128.59 (C-PPh_3), 128.59 (C-16), 127.6, 127.56 (C-23,-25), 127.45 (C-23,-29), 127.18 (C-3), 119.00 (C-18), 91.69 (C-9,-11), 74.79 (C-8,-12), 48.75 (C-7), 34.90 (C-19), 34.65 (C-20), 30.77 (C-33), 30.61 (C-34), 20.2 (C-36), 20.08 (C-35,-37), 20.05 (C-38,-40), 20.07 (C-39) ppm; $^{31}P\{^1H\}$ NMR (202 MHz, [D8]THF, 299 K): $\delta = 15.07$ ppm; ^{19}F NMR (162 MHz, [D8]THF, 299 K): $\delta = -79.49$ ppm (s, NTf_2-anion); UV/Vis(THF): λ (ε): 362 (8400), 417 (11 000), 524 (7400), 742 nm (2300 $mol^{-1} dm^3 cm^{-1}$); elemental analysis calcd (%) for $C_{82}H_{79}Ni_2P_2S_4NF_6O_4$: C 62.97, H 5.09, S 8.20, N 0.90; found: C 62.72, H 5.36, S 7.68, N 0.89. [a] Partially obscured by resonances of PPh_3 ligands

Preparation of $[\mathbf{3_{Mes}}$-$\mathbf{PCy_3}]\mathbf{NTf_2}$: A solution of $\mathbf{2}_{Mes}$-PCy_3 (50 mg, 0.038 mmol) in THF (8 mL) was cooled down to $-15\,^\circ C$ in an ice/NaCl bath and an ice-cooled solution of $FcNTf_2$ (17 mg, 0.038 mmol) in THF (8 mL) was cannulated to the complex. Instantaneously, the color of the solution turned yellow brown and the reaction mixture was stirred for 30 min in the cooling bath and then an additional 30 min. at room temperature. The solvent was removed under vacuum and the product was washed with toluene and recrystallized by slow diffusion of hexane vapor into a concentrated solution of $[\mathbf{3}_{Mes}$-$PCy_3]NTf_2$ in THF, which provided 37 mg (0.023 mmol, 61 %) of yellow brown crystals. UV/Vis(THF): λ (ε): 310 (13 600), 353 (13 300), 403 (13 100), 490 (5100), 580 (3500), 814 nm (1600 $mol^{-1} dm^3 cm^{-1}$); $\mu_{eff} = 2.3$ (Evans method, 278–318 K, $CDCl_3$ containing HMDS); elemental analysis calcd (%) for $C_{82}H_{114}Ni_2P_2S_4NF_6O_4$: C 61.58, H 7.18, S 8.02, N 0.88; found: C 61.14, H 7.24, S 7.74, N 0.91.

Cyclic voltammetry

Stock solutions of compounds $\mathbf{1}_R$-PMe_3, $\mathbf{2}_{Mes}$-L, and $\mathbf{3}_R$-L were prepared in 0.1 M nBu_4NPF_6/1,2-DFB in 1 mL volumetric flasks, concentrations being in the range of $4–8 \times 10^{-3}$ M· The electrochemical cell containing the GC working, Pt-counter and a Pt-wire electrode was evacuated and backfilled with argon three times, and charged with 8 mL of electrolyte solution by syringe. The Ag/ Ag^+-reference electrode in MeCN was connected to the cell by a Haber-Luggin capillary filled with electrolyte solution and was connected by a 0,01-µF capacitor to the Pt-wire electrode completing the double-reference electrode system. After a stable resting potential was reached under open circuit conditions, background CV scans in the appropriate potential range were run on the electrolyte solution at sweep rates of 20, 50, 100, 200, 500, 1000, 5000, and 10 000 $mV s^{-1}$, and the correction for overall cell resistance was applied manually on the potentiostat. Sample aliquots (25–50 µL range) were added to the cell through a septum cap using a gastight 100 µL syringe, and CV data were collected at aforementioned sweep rates.

Acknowledgements

A.B. and F.K. are indebted to the Fonds der Chemischen Industrie and the Eliteprogramme for Postdocs of the Baden-Württemberg Stiftung for financial support. We are grateful to Dr. K. Eichele for assistance with and discussion of NMR data, Dipl. Chem. Nicole Mews for the preparation of $[Fc]NTf_2$, and Umicore AG & Co. KG, Hanau, Germany, for a generous donation of $(tBu_3P)_2Pd$.

Keywords: binuclear complexes · ligand cooperativity · nickel · proton reduction · thiophenolato ligands

[1] a) J. R. McKone, S. C. Marinescu, B. S. Brunschwig, J. R. Winkler, H. B. Gray, *Chem. Sci.* **2014**, *5*, 865 – 878; b) D. Z. Zee, T. Chantarojsiri, J. R. Long, C. J. Chang, *Acc. Chem. Res.* **2015**, *48*, 2027 – 2036; c) R. M. Bullock, A. M. Appel, M. L. Helm, *Chem. Commun.* **2014**, *50*, 3125 – 3143; d) V. Artero, M. Fontecave, *Coord. Chem. Rev.* **2005**, *249*, 1518 – 1535.

[2] a) M. L. Helm, M. P. Stewart, R. M. Bullock, M. R. DuBois, D. L. DuBois, *Science* **2011**, *333*, 863 – 866; b) T. Liu, S. Chen, M. J. O'Hagan, M. Rakowski DuBois, R. M. Bullock, D. L. DuBois, *J. Am. Chem. Soc.* **2012**, *134*, 6257 –

6272; c) M. P. Stewart, M.-H. Ho, S. Wiese, M. L. Lindstrom, C. E. Thogerson, S. Raugei, R. M. Bullock, M. L. Helm, *J. Am. Chem. Soc.* **2013**, *135*, 6033 – 6046; d) Z. Han, R. Eisenberg, *Acc. Chem. Res.* **2014**, *47*, 2537 – 2544; e) T. Nakae, M. Hirotsu, I. Kinoshita, *Organometallics* **2015**, *34*, 3988 – 3997; f) N. D. Loewen, E. J. Thompson, M. Kagan, C. L. Banales, T. W. Myers, J. C. Fettinger, L. A. Berben, *Chem. Sci.* **2016**, *7*, 2728 – 2735.

[3] E. I. Solomon, S. I. Gorelsky, A. Dey, *J. Comput. Chem.* **2006**, *27*, 1415 – 1428.

[4] Z. Huang, W. Luo, L. Ma, M. Yu, X. Ren, M. He, S. Polen, K. Click, B. Garrett, J. Lu, K. Amine, C. Hadad, W. Chen, A. Asthagiri, Y. Wu, *Angew. Chem. Int. Ed.* **2015**, *54*, 15181 – 15185; *Angew. Chem.* **2015**, *127*, 15396 – 15400.

[5] a) M. Y. Darensbourg, W. F. Liaw, C. G. Riordan, *J. Am. Chem. Soc.* **1989**, *111*, 8051 – 8052; b) S. Kaur-Ghumaan, L. Schwartz, R. Lomoth, M. Stein, S. Ott, *Angew. Chem. Int. Ed.* **2010**, *49*, 8033 – 8036; *Angew. Chem.* **2010**, *122*, 8207 – 8211; c) R. Zaffaroni, T. B. Rauchfuss, D. L. Gray, L. De Gioia, G. Zampella, *J. Am. Chem. Soc.* **2012**, *134*, 19260 – 19269.

[6] D. Sellmann, R. Prakash, F. W. Heinemann, M. Moll, M. Klimowicz, *Angew. Chem. Int. Ed.* **2004**, *43*, 1877 – 1880; *Angew. Chem.* **2004**, *116*, 1913 – 1916.

[7] C. S. Letko, J. A. Panetier, M. Head-Gordon, T. D. Tilley, *J. Am. Chem. Soc.* **2014**, *136*, 9364 – 9376.

[8] D. Sellmann, J. Kaeppler, M. Moll, *J. Am. Chem. Soc.* **1993**, *115*, 1830 – 1835.

[9] A. Zarkadoulas, M. J. Field, C. Papatriantafyllopoulou, J. Fize, V. Artero, C. A. Mitsopoulou, *Inorg. Chem.* **2016**, *55*, 432 – 444.

[10] a) H. Ogata, K. Nishikawa, W. Lubitz, *Nature* **2015**, *520*, 571 – 574; b) W. Lubitz, H. Ogata, O. Rüdiger, E. Reijerse, *Chem. Rev.* **2014**, *114*, 4081 – 4148; c) E. Bouwman, J. Reedijk, *Coord. Chem. Rev.* **2005**, *249*, 1555 – 1581.

[11] a) X. Zhao, I. P. Georgakaki, M. L. Miller, J. C. Yarbrough, M. Y. Darensbourg, *J. Am. Chem. Soc.* **2001**, *123*, 9710 – 9711; b) A. Jablonskytė, L. R. Webster, T. R. Simmons, J. A. Wright, C. J. Pickett, *J. Am. Chem. Soc.* **2014**, *136*, 13038 – 13044; c) T. B. Rauchfuss, *Acc. Chem. Res.* **2015**, *48*, 2107 – 2116.

[12] a) W. Zhu, A. C. Marr, Q. Wang, F. Neese, D. J. E. Spencer, A. J. Blake, P. A. Cooke, C. Wilson, M. Schröder, *Proc. Natl. Acad. Sci. USA* **2005**, *102*, 18280 – 18285; b) B. E. Barton, T. B. Rauchfuss, *J. Am. Chem. Soc.* **2010**, *132*, 14877 – 14885; c) K. Weber, T. Krämer, H. S. Shafaat, T. Weyhermüller, E. Bill, M. van Gastel, F. Neese, W. Lubitz, *J. Am. Chem. Soc.* **2012**, *134*, 20745 – 20755.

[13] a) P. Rigo, M. Bressan, M. Basato, *Inorg. Chem.* **1979**, *18*, 860 – 863; b) T. L. James, L. Cai, M. C. Muetterties, R. H. Holm, *Inorg. Chem.* **1996**, *35*, 4148 – 4161; c) E. S. Wiedner, H. J. S. Brown, M. L. Helm, *J. Am. Chem. Soc.* **2016**, *138*, 604 – 616; d) E. S. Rountree, J. L. Dempsey, *J. Am. Chem. Soc.* **2015**, *137*, 13371 – 13380; e) P.-A. Jacques, V. Artero, J. Pécaut, M. Fontecave, *Proc. Natl. Acad. Sci. USA* **2009**, *106*, 20627 – 20632; f) O. Pantani, E. Anxolabéhère-Mallart, A. Aukauloo, P. Millet, *Electrochem. Commun.* **2007**, *9*, 54 – 58; g) O. R. Luca, S. J. Konezny, J. D. Blakemore, D. M. Colosi, S. Saha, G. W. Brudvig, V. S. Batista, R. H. Crabtree, *New J. Chem.* **2012**, *36*, 1149 – 1152; h) R. Tatematsu, T. Inomata, T. Ozawa, H. Masuda, *Angew. Chem. Int. Ed.* **2016**, *55*, 5247 – 5250; i) Y. Han, H. Fang, H. Jing, H. Sun, H. Lei, W. Lai, R. Cao, *Angew. Chem. Int. Ed.* **2016**, *55*, 5457 – 5462; *Angew. Chem.* **2016**, *128*, 5547 – 5552; j) H. Shao, S. K. Muduli, P. D. Tran, H. S. Soo, *Chem. Commun.* **2016**, *52*, 2948 – 2951; k) S. Ramakrishnan, S. Chakraborty, W. W. Brennessel, C. E. D. Chidsey, W. D. Jones, *Chem. Sci.* **2016**, *7*, 117 – 127; l) O. R. Luca, S. J. Konezny, E. K. Paulson, F. Habib, K. M. Luthy, M. Murugesu, R. H. Crabtree, V. S. Batista, *Dalton Trans.* **2013**, *42*, 8802 – 8807; m) O. R. Luca, J. D. Blakemore, S. J. Konezny, J. M. Praetorius, T. J. Schmeier, G. B. Hunsinger, V. S. Batista, G. W. Brudvig, N. Hazari, R. H. Crabtree, *Inorg. Chem.* **2012**, *51*, 8704 – 8709; n) P. Zhang, M. Wang, Y. Yang, D. Zheng, K. Han, L. Sun, *Chem. Commun.* **2014**, *50*, 14153 – 14156; o) W. Zhang, J. Hong, J. Zheng, Z. Huang, J. Zhou, R. Xu, *J. Am. Chem. Soc.* **2011**, *133*, 20680 – 20683; p) A. Begum, G. Moula, S. Sarkar, *Chem. Eur. J.* **2010**, *16*, 12324 – 12327.

[14] a) J. P. Collin, A. Jouaiti, J. P. Sauvage, *Inorg. Chem.* **1988**, *27*, 1986 – 1990; b) S. Pfirrmann, C. Limberg, B. Ziemer, *Dalton Trans.* **2008**, 6689 – 6691; c) T. Matsumoto, T. Nagahama, J. Cho, T. Hizume, M. Suzuki, S. Ogo, *Angew. Chem. Int. Ed.* **2011**, *50*, 10578 – 10580; *Angew. Chem.* **2011**, *123*, 10766 – 10768; d) H. Gehring, R. Metzinger, C. Herwig, J. Intemann, S. Harder, C. Limberg, *Chem. Eur. J.* **2013**, *19*, 1629 – 1636; e) A. Mondragón, M. Flores-Alamo, P. R. Martínez-Alanis, G. Aullón, V. M. Ugalde-Saldívar, I. Castillo, *Inorg. Chem.* **2015**, *54*, 619 – 627.

[15] a) J. J. Eisch, A. M. Piotrowski, K. I. Han, C. Kruger, Y. H. Tsay, *Organometallics* **1985**, *4*, 224 – 231; b) C. A. Laskowski, G. L. Hillhouse, *Organometallics* **2009**, *28*, 6114 – 6120; c) A. Velian, S. Lin, A. J. M. Miller, M. W. Day, T. Agapie, *J. Am. Chem. Soc.* **2010**, *132*, 6296 – 6297; d) R. Beck, S. A. Johnson, *Chem. Commun.* **2011**, *47*, 9233 – 9235; e) T. J. Steiman, C. Uyeda, *J. Am. Chem. Soc.* **2015**, *137*, 6104 – 6110; f) S. Pal, C. Uyeda, *J. Am. Chem. Soc.* **2015**, *137*, 8042 – 8045; g) Y.-Y. Zhou, C. Uyeda, *Angew. Chem. Int. Ed.* **2016**, *55*, 3171 – 3175.

[16] T. L. James, D. M. Smith, R. H. Holm, *Inorg. Chem.* **1994**, *33*, 4869 – 4877.

[17] a) H. Wadepohl, *Angew. Chem. Int. Ed. Engl.* **1992**, *31*, 247 – 262; *Angew. Chem.* **1992**, *104*, 253 – 268; b) T. Murahashi, H. Kurosawa, *Coord. Chem. Rev.* **2002**, *231*, 207 – 228.

[18] a) G. Bai, P. Wei, D. W. Stephan, *Organometallics* **2005**, *24*, 5901 – 5908; b) M. Ito, T. Matsumoto, K. Tatsumi, *Inorg. Chem.* **2009**, *48*, 2215 – 2223; c) C. Jones, C. Schulten, L. Fohlmeister, A. Stasch, K. S. Murray, B. Moubaraki, S. Kohl, M. Z. Ertem, L. Gagliardi, C. J. Cramer, *Chem. Eur. J.* **2011**, *17*, 1294 – 1303; d) J. Wu, A. Nova, D. Balcells, G. W. Brudvig, W. Dai, L. M. Guard, N. Hazari, P.-H. Lin, R. Pokhrel, M. K. Takase, *Chem. Eur. J.* **2014**, *20*, 5327 – 5337.

[19] S. Lin, M. W. Day, T. Agapie, *J. Am. Chem. Soc.* **2011**, *133*, 3828 – 3831.

[20] a) S. Suseno, K. T. Horak, M. W. Day, T. Agapie, *Organometallics* **2013**, *32*, 6883 – 6886; b) K. T. Horak, S. Lin, J. Rittle, T. Agapie, *Organometallics* **2015**, *34*, 4429 – 4432.

[21] S. Lin, D. E. Herbert, A. Velian, M. W. Day, T. Agapie, *J. Am. Chem. Soc.* **2013**, *135*, 15830 – 15840.

[22] K. T. Horak, A. Velian, M. W. Day, T. Agapie, *Chem. Commun.* **2014**, *50*, 4427 – 4429.

[23] J. A. Buss, T. Agapie, *Nature* **2016**, *529*, 72 – 75.

[24] F. Koch, H. Schubert, P. Sirsch, A. Berkefeld, *Dalton Trans.* **2015**, *44*, 13315 – 13324.

[25] CCDC 1483732 to 1483736 contain the supplementary crystallographic data for this paper. These data are provided free of charge by The Cambridge Crystallographic Data Centre. See the Supporting Information, Tables S3 – S4 for details.

[26] J. S. Kim, J. H. Reibenspies, M. Y. Darensbourg, *J. Am. Chem. Soc.* **1996**, *118*, 4115 – 4123.

[27] Q. Wang, A. J. Blake, E. S. Davies, E. J. L. McInnes, C. Wilson, M. Schroder, *Chem. Commun.* **2003**, 3012 – 3013.

[28] H. J. Krueger, R. H. Holm, *Inorg. Chem.* **1989**, *28*, 1148 – 1155.

[29] a) D. M. D'Alessandr, F. R. Keene, *Chem. Rev.* **2006**, *106*, 2270 – 2298; b) M. S. Ziegler, D. S. Levine, K. V. Lakshmi, T. D. Tilley, *J. Am. Chem. Soc.* **2016**, *138*, 6484 – 6491.

[30] a) G. Garrido, E. Koort, C. Ràfols, E. Bosch, T. Rodima, I. Leito, M. Rosés, *J. Org. Chem.* **2006**, *71*, 9062 – 9067; b) G. Garrido, M. Rosés, C. Ràfols, E. Bosch, *J. Solution Chem.* **2008**, *37*, 689 – 700.

[31] K. W. Kramarz, J. R. Norton, in *Progress in Inorganic Chemistry*, Wiley, **2007**, pp. 1 – 65.

[32] T.-H. Chao, J. H. Espenson, *J. Am. Chem. Soc.* **1978**, *100*, 129 – 133.

[33] O. Dahl, *Acta Chemical Scandinavica* **1969**, *23*, 2342 – 2354.

[34] D. J. Krysan, P. B. Mackenzie, *J. Org. Chem.* **1990**, *55*, 4229 – 4230.

[35] D. F. Evans, *J. Chem. Soc.* **1959**, 2003 – 2005.

[36] G. A. Bain, J. F. Berry, *J. Chem. Educ.* **2008**, *85*, 532.

[37] M. Kumar, R. Gupta, in *Landolt-Börnstein, New Series II, Vol. 27B: Diamagnetic Susceptibility of Organic Compounds, Oils, Paraffins and Polyethylenes* (Ed.: R. R. Gupta), Springer, Heidelberg, **2008**.

[38] L. J. Farrugia, *J. Appl. Crystallogr.* **1999**, *32*, 837.

[39] a) G. M. S. C. B. Hübschle, B. Dittrich, *J. Appl. Crystallogr.* **2011**, *44*, 1281 – 1284; b) G. M. Sheldrick, *Acta Crystallogr. Sect. A* **2008**, *64*, 112 – 122.

[40] A. L. Speck, *Acta Crystallogr. Sect. D* **2009**, *65*, 148 – 155.

[41] L. J. Farrugia, *J. Appl. Crystallogr.* **2012**, *45*, 849 – 854.

Received: July 28, 2016

FULL PAPER

Acids' choice: The redox and acid–base properties of binuclear complexes of nickel from 1,4-terphenyldithiophenol ligands are reported. Donor/acceptor contributions to metal–ligand bonding flexibly adjust to stabilize different redox states at the metals, which is relevant for redox reactions like proton reduction. Proton transfer to the [S_2Ni_2] core and Ni–H bond formation are kinetically favored over the thermodynamically favored yet unproductive proton transfer to ligand (see scheme).

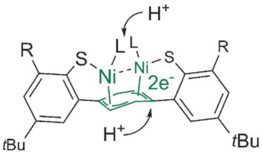

Binuclear Complexes

F. Koch, A. Berkefeld, H. Schubert, C. Grauer*

■■ – ■■

Redox and Acid–Base Properties of Binuclear 4-Terphenyldithiophenolate Complexes of Nickel